JOURNAL OF BACTERIOLOGY, Feb. 1983, p. 1027–1037
0021-9193/83/021027-11$02.00/0

Vol. 153, No. 2

Identification and Localization of Enzymes of the Fumarate Reductase and Nitrate Respiration Systems of *Escherichia coli* by Crossed Immunoelectrophoresis

JAN VAN DER PLAS,[1] KLAAS J. HELLINGWERF,[1] HENDRIK G. SEIJEN,[2] JOHN R. GUEST,[3] JOHN H. WEINER,[4] AND WIL N. KONINGS[1]*

Department of Microbiology, University of Groningen, 9751 NN Haren,[1] and Department of Histology, University of Groningen, 9713 EZ Groningen,[2] The Netherlands; Department of Microbiology, University of Sheffield, Sheffield S10 2TN, England[3]; and Department of Biochemistry, University of Alberta, Edmonton T6G 2H7, Canada[4]

Received 12 July 1982/Accepted 25 October 1982

Crossed immunoelectrophoresis was used to analyze the components of membrane vesicles of anaerobically grown *Escherichia coli*. The number of precipitation lines in the crossed immunoelectrophoresis patterns of membrane vesicles isolated from *E. coli* grown anaerobically on glucose plus nitrate and on glycerol plus fumarate were 83 and 70, respectively. Zymogram staining techniques were used to identify immunoprecipitates corresponding to nitrate reductase, formate dehydrogenase, fumarate reductase, and glycerol-3-phosphate dehydrogenase in crossed immunoelectrophoresis reference patterns. The identification of fumarate reductase by its succinate oxidizing activity was confirmed with purified enzyme and with mutants lacking or overproducing this enzyme. In addition, precipitation lines were found for hydrogenase, cytochrome oxidase, the membrane-bound ATPase, and the dehydrogenases for succinate, malate, dihydroorotate, D-lactate, 6-phosphogluconate, and NADH. Adsorption experiments with intact and solubilized membrane vesicles showed that fumarate reductase, hydrogenase, glycerol-3-phosphate dehydrogenase, nitrate reductase, and ATPase are located at the inner surface of the cytoplasmic membrane; on the other hand, the results suggest that formate dehydrogenase is a transmembrane protein.

Facultative anaerobic bacteria such as *Escherichia coli* are able to generate metabolic energy under anaerobic conditions by substrate-level phosphorylation, by end-product efflux (41), and also by energy transduction of anaerobic electron transfer systems (25). In *E. coli*, two anaerobic electron transfer systems are found: the fumarate reductase and the nitrate respiration systems (18, 25, 27, 40). The capacity of these two electron transfer systems to generate an electrochemical potential gradient for protons ($\Delta\tilde{\mu}_{H^+}$) across the cytoplasmic membrane has been determined. A progressively increasing $\Delta\tilde{\mu}_{H^+}$ can be generated in *E. coli* when the electron acceptor is changed from fumarate via nitrate to oxygen (19). Consistent with this is the observation that electron transfer in the nitrate and fumarate reduction systems can effectively energize solute transport in the membrane vesicles of *E. coli* (2). Further bioenergetic characterization requires an evaluation of the number of protons translocated across the membrane with each pair of electrons traversing the electron transfer systems. Values of two and four protons per electron pair have been reported for the fumarate reductase and nitrate respiration systems, respectively (11, 31).

Information concerning the topography of the respective components of the electron transfer systems in the cytoplasmic membrane is required to interpret these results. In *E. coli*, the location of the enzymes catalyzing the first and terminal reactions in these anaerobic electron transfer systems is still not firmly established. This has now been investigated by crossed immunoelectrophoresis, a technique which can in principle yield information about all the antigenic components of the membrane. This technique has been used to analyze the orientation of membrane vesicles of aerobically grown *E. coli* (32) and subsequently to locate membrane components in the cytoplasmic membranes of *E. coli* and other organisms (1, 9, 34).

The fumarate reductase and nitrate respiration systems of *E. coli* have been studied extensively, and properties relevant to this investigation are summarized as follows.

(i) The fumarate reductase system (18, 20, 25,

27) is composed of a dehydrogenase (e.g., that of NADH, glycerol-3-phosphate, or formate) or hydrogenase, menaquinone, cytochrome *b*, and fumarate reductase. Its expression is highly regulated, induced under anaerobic conditions, and repressed by electron acceptors such as O_2 and nitrate. A complex containing the intact fumarate reductase system has been isolated from the membranes of *E. coli* (30). Evidence that fumarate reductase is located at the inner surface of the cytoplasmic membrane has been presented for several organisms (27). In *E. coli*, fumarate has to be translocated across the cytoplasmic membrane before it is reduced by fumarate reductase (17). Furthermore, spheroplasts do not oxidize many artificial electron mediators via the fumarate reductase system unless the cytoplasmic membrane is disrupted (21). Fumarate reductase has been isolated in a pure form (7) and shown to be a flavoprotein (43). In addition to fumarate reductase, *E. coli* contains a second enzyme that catalyzes the interconversion of fumarate and succinate (20): succinate dehydrogenase, which is also a flavoprotein.

(ii) The nitrate respiration system of *E. coli* contains NADH dehydrogenase or formate dehydrogenase and a cytochrome *b*, ubiquinone, and a complex of a second cytochrome *b* with nitrate reductase (18, 25, 36, 40). Nitrate reductase has been purified to homogeneity and extensively characterized with respect to subunit composition and cofactor requirements. Of its three subunits (α, β, and γ), the γ subunit is a cytochrome *b* (40). Many techniques have been used to assay the membrane orientation of nitrate reductase in intact cells, spheroplasts, membrane vesicles, and inverted vesicles, e.g., labeling with ^{125}I-lactoperoxidase (3), kinetic analysis of reduction and oxidation of different artificial electron acceptors or donors (21), and fluorescent antibody binding (13). Although these methods have occasionally led to conflicting models (compare references 21 and 22), it is now generally accepted (22, 40) that the α and β subunits of nitrate reductase are both exposed to the cytoplasm and that one or both contain the nitrate-reactive sites. The γ subunit is the only component of the nitrate reductase complex which can be reached from the periplasmic side of the membrane.

MATERIALS AND METHODS

Growth of cells. *E. coli* ML308-225 (*lacIZY*$^+$*A*$^+$) was grown anaerobically at 37°C on minimal medium A supplemented with 0.1% yeast extract as described previously (2). The carbon sources, electron donors, and trace metals were either 0.5% glucose–50 mM potassium nitrate–1 μM sodium selenate–1 μM sodium molybdate or 0.5% glycerol–10 mM sodium fumarate. Vesicles derived from cells grown on these media will be referred to as glucose-nitrate and glycerol-fumarate vesicles, respectively.

E. coli K-12 strain JRG531 (*frdA3*), an *frd* amber mutant, was derived from strain JRG653 (*gal trpA9761 trpR iclR rpsL*), formerly WGAS (39). Strain JRG1030 (formerly G400), an ampicillin-hyperresistant strain which bears multiple gene duplications in the *ampC* (β-lactamase) gene region of the chromosome and overproduces fumarate reductase, was derived from strain JRG997 (*ilv metB ampA1*) (5). These strains were grown on 0.5% glucose–10 mM sodium fumarate in the medium described above.

To get good amplification of fumarate reductase in strain JRG1030, a relatively large inoculum (1/25 of the batch volume) of aerobic cells grown on L-broth with 400 μg of ampicillin per ml (5) was used. Anaerobic growth without ampicillin was for 3 h. This procedure maintains the selection for the gene duplications and allows anaerobic derepression of fumarate reductase.

Preparation of membrane vesicles. Membrane vesicles were prepared by the method of Konings and Kaback (26) and were stored in liquid nitrogen.

Preparation of Triton X-100 extracts. Membrane vesicles, suspended after centrifugation (48,000 × *g*, 4°C, 30 min) in 50 mM Tris-hydrochloride 8.6) containing 5 mM EDTA and 9% (vol/vol) Triton X-100 to a protein concentration of approximately 10 mg/ml, were incubated for 1 h at 20°C. This suspension was centrifuged (48,000 × *g*, 4°C, 60 min), and the supernatants (about 7 mg of protein per ml) were stored in 50-μl portions in liquid nitrogen.

Isolation of antibodies. Antibodies against the glucose-nitrate and glycerol-fumarate membrane vesicle proteins of *E. coli* ML308-225 were raised in *Chinchilla giganta* rabbits (9), and immunoglobulins were isolated essentially as described before (23). The antibodies were concentrated (40 to 140 mg of protein per ml) either by ammonium sulfate precipitation (at 50% saturation) or on a Diaflow XM50 filter (Amicon, Lexington, Mass.) and were stored at −20°C after dialysis against 20 mM barbital hydrochloride buffer, pH 8.6.

Crossed immunoelectrophoresis. Crossed immunoelectrophoresis was carried out in 3.2 ml of 1% agarose on glass plates (5 by 5 cm) in a water-cooled electrophoresis chamber (Holm-Nielsen, Copenhagen, Denmark) as described previously (9). The electric field strength applied was 2.5 V/cm for 3 h and 1.5 V/cm for 16 to 18 h in the first and second dimensions, respectively. The anodes are shown at the left and at the top of the figures for all experiments.

Zymogram staining. Precipitation lines in the crossed immunoelectrophoresis patterns were identified by the following zymogram staining techniques.

(i) The membrane-bound (Ca^{2+}, Mg^{2+}) ATPase was identified with Mg^{2+}-ATP by the method of Owen and Salton (35).

(ii) The dehydrogenases for glycerol-3-phosphate, dihydroorotate, D-lactate, malate, NADH, and 6-phosphogluconate and the succinate oxidizing activities were identified as described (33), except that KCN was omitted, and phenazine ethosulfate was used instead of phenazine methosulfate when needed (12). Formate dehydrogenase was identified by incubating immunoplates in a mixture containing 18 ml of 50 mM potassium phosphate (pH 7.3), 2.0 ml of 1 M sodium formate (pH 7.3), 0.5 mg of phenazine ethosulfate, and

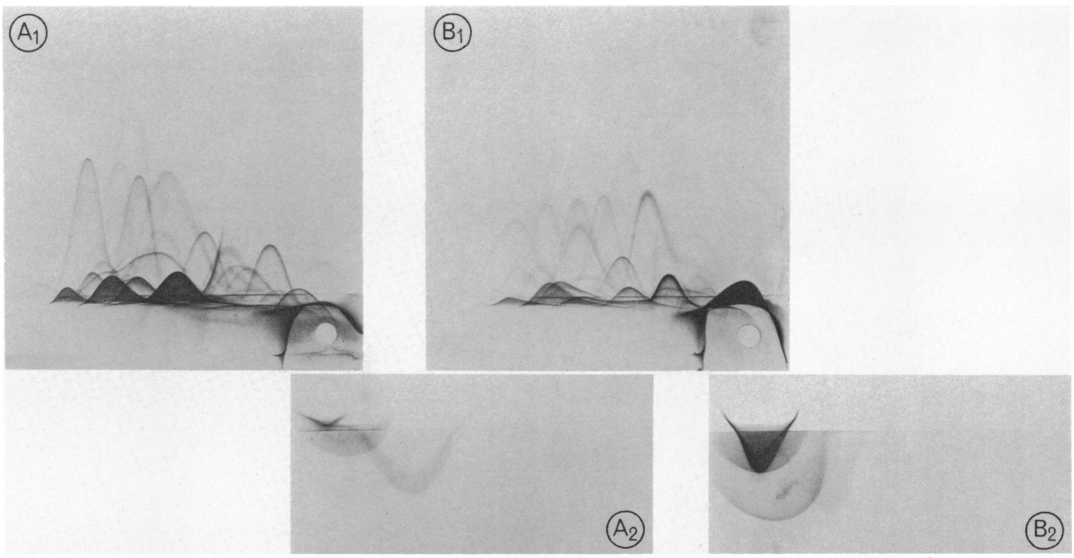

FIG. 1. Typical crossed immunoelectropherogram of EDTA–Triton X-100 extracts of glucose-nitrate (A) and glycerol-fumarate (B) membrane vesicles. In each assay, 46 (A) or 51 (B) μg of vesicle protein was analyzed by crossed immunoelectrophoresis against 14 (A1) or 28 (A2) mg of anti-glucose-nitrate immunoglobulins and 8 (B1) or 32 (B2) mg of anti-glycerol-fumarate immunoglobulins. To detect strongly basic membrane proteins, the application well was transferred from the lower right-hand to the upper left-hand corner (A2 and B2).

4 mg of tetranitro blue tetrazolium. Incubation was carried out at 30°C in the dark for appropriate times from 30 min for glycerol-3-phosphate dehydrogenase to 48 h for formate and succinate dehydrogenases.

(iii) For nitrate reductase, the procedure was similar to that described by Lund and DeMoss (29) for polyacrylamide gels. Gels were photographed immediately after the apppearance of a clear peak area (usually within 10 min). When hydrogenase activity is present, this precipitation line decolorizes before the nitrate is added. As an alternative, the nitrate reductase region was stained pink by a modification of the colorimetric assay for nitrite. For this the reaction mixture contained 60 mg of methyl viologen, 50 mg of sodium dithionite, 3.75 ml of a 2% (wt/vol) solution of *N*-(1-naphthyl)ethylenediamine, 7.5 ml of 1% (wt/vol) sulfanilamide, and 14 ml of potassium phosphate (pH 7.2). After allowing enzymatic nitrite formation, the immunoplate was transferred to a 1 N HCl solution to stop the reaction and to initiate the development of the pink color.

(iv) Fumarate reductase was routinely detected by its ability to oxidize succinate (see above, section ii) and also by the procedure of Lund and DeMoss (29) for nitrate reductase, except that nitrate was replaced by sodium fumarate (0.4 ml, 0.5 M). Again, hydrogenase activity may become visible before the addition of substrate.

(v) Hydrogenase activity was detected as described above (sections iii and iv) or by the method of Graham et al. (15) but with tetranitro blue tetrazolium instead of 2,3,5-triphenyltetrazolium chloride and with incubation under an atmosphere of hydrogen provided by a GasPak anaerobic system (BBL Microbiology Systems, Cockeysville, Md.).

(vi) Heme-associated peroxidase activity was detected by the method of Thomas et al. (42).

(vii) Cytochrome oxidase activity was stained as described by Burstone (4).

Adsorption experiments. Adsorption experiments of anti-glucose-nitrate and anti-glycerol-fumarate vesicle immunoglobulins were performed with intact or disrupted vesicles essentially as described previously (9). After centrifugation (48,000 × *g*, 4°C, 30 min), glucose-nitrate and glycerol-fumarate vesicles were either suspended at 5 mg of protein per ml in 50 mM Tris-hydrochloride (pH 8.6) and kept at 4°C (intact vesicles) or were suspended at the same concentration in the same buffer supplemented with 5 mM EDTA–4.5% (vol/vol) Triton X-100 and incubated for 60 min at 20°C (disrupted vesicles).

Adsorption experiments with glucose-nitrate vesicles were performed by adding 0.4-ml samples of anti-glucose-nitrate immunoglobulins (containing 28 mg of protein) to 0 to 0.6 ml of intact or disrupted vesicles. Tris-hydrochloride buffer (50 mM, pH 8.6) was added to give a final volume of 1.0 ml.

Adsorption experiments with glycerol-fumarate vesicles were performed by adding 0.28-ml samples of anti-glycerol-fumarate immunoglobulins (39 mg of protein) to 0 to 0.72 ml of intact or 0 to 0.36 ml of disrupted vesicles. Tris-hydrochloride buffer was again added to give a final volume of 1.0 ml. After incubation for 60 min at 20°C with frequent shaking, the absorption mixtures were centrifuged as above, and the supernatant fractions containing the residual immunoglobulins were stored at −20°C. For each crossed immunoelectrophoresis experiment, 50 to 200 μl of one of these suspensions was incorporated in the second-dimension agarose gel. The peak area of indi-

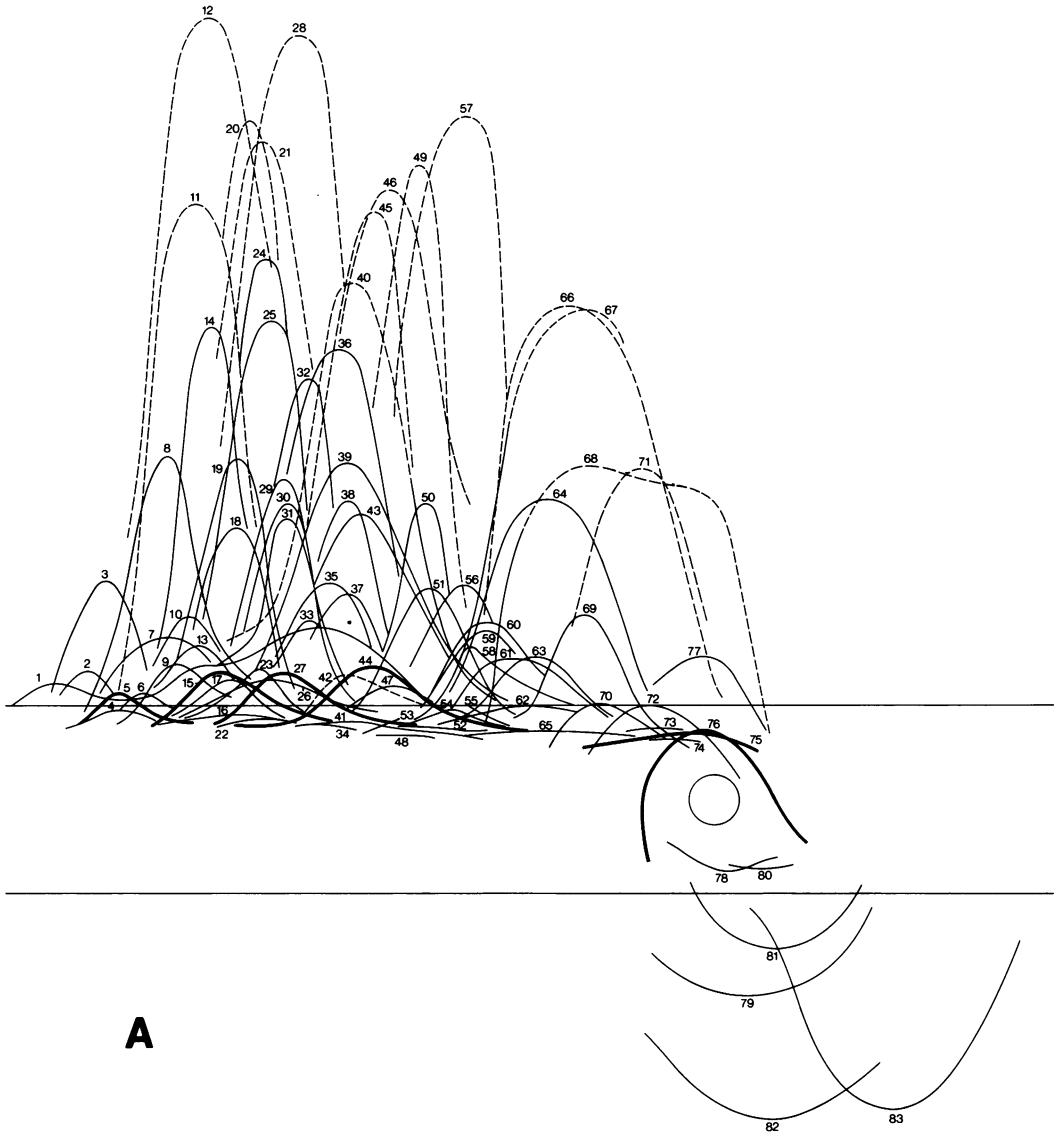

FIG. 2. Crossed immunoelectrophoresis reference patterns of glucose-nitrate and glycerol-fumarate membrane vesicles. Schematic representation of the crossed immunoelectrophoresis patterns of EDTA–Triton X-100 extracts of glucose-nitrate (A) and glycerol-fumarate (B) membrane vesicles were deduced from an extensive series of immunoplates run with 46 (A) or 51 (B) μg of antigen and antibody concentrations varying from 0.7 to 52.5 (A) and from 0.8 to 52.0 (B) mg. The immunoprecipitates are numbered in order of decreasing electrophoretic mobility of the peak maxima. The thickness of line reflects the intensity of the Coomassie brilliant blue stain observed for the different immunoprecipitates. Dotted lines denote precipitates detected only with more than 17.5 (A) or 8.0 (B) mg of antibody in the second-dimension gel.

vidual immunoprecipitates was determined after 10-fold optical enlargement with a Hewlett-Packard integrator (Hewlett-Packard Co., Palo Alto, Calif.).

Purification of fumarate reductase. Fumarate reductase was purified as described by Dickie and Weiner (7). The enzyme solution containing about 4 mg of protein per ml was diluted in 5 mM EDTA–9% (vol/vol) Triton X-100–50 mM Tris-hydrochloride (pH 8.6) to a final concentration of 1 mg/ml and was extensively dialyzed against this buffer to bring the enzyme to the same conditions as the solubilized membrane vesicle protein.

Protein determination. Protein was determined by the method of Lowry et al. (28) as modified by Dully and Grieve (8). Bovine serum albumin was used as a standard.

Materials. Agarose and Triton X-100 were obtained from Miles Laboratories, Inc. (Elkhart, Ind.) and

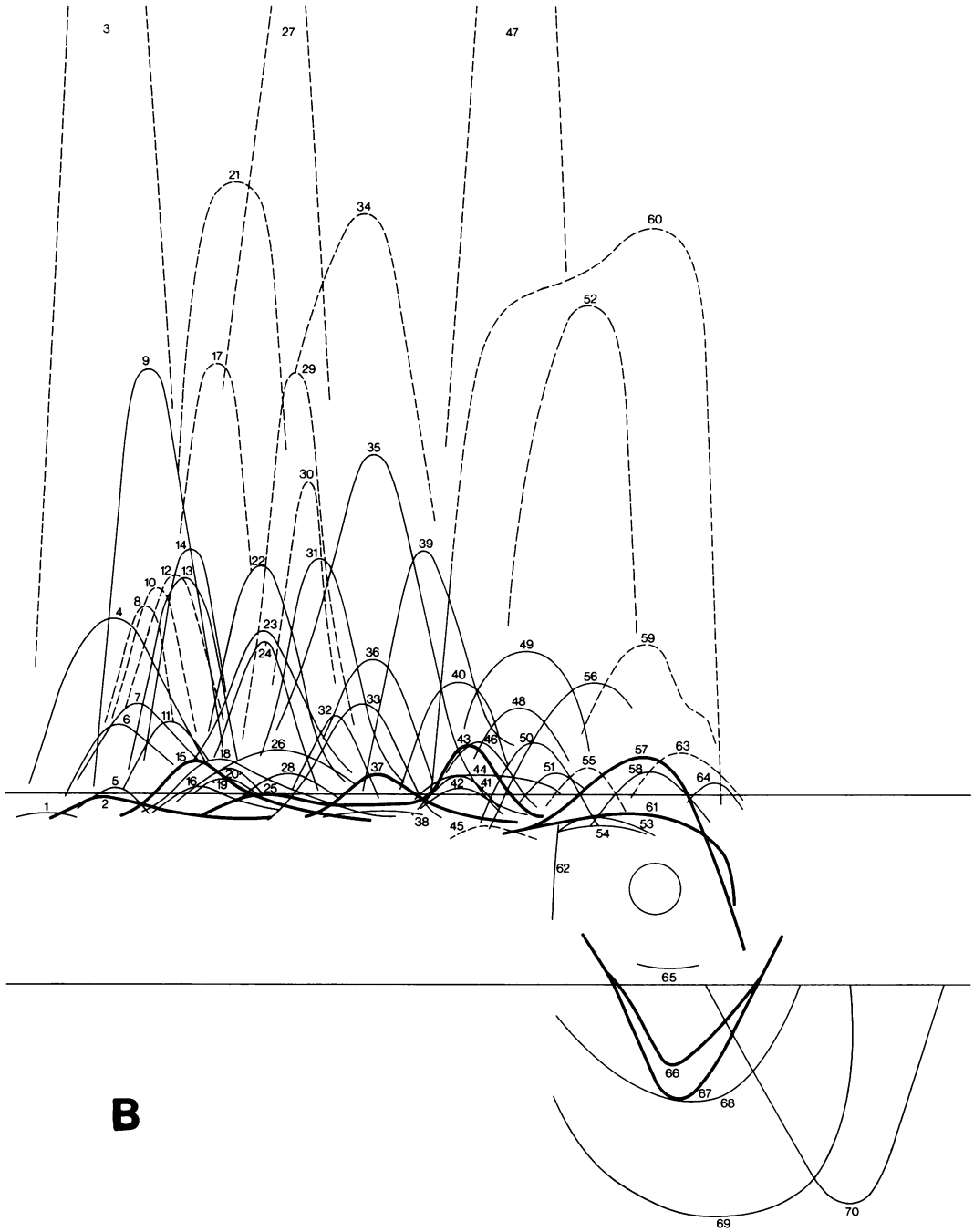

BDH (Poole, United Kingdom), respectively. All other materials were reagent grade and obtained from commercial sources.

RESULTS AND DISCUSSION

Crossed immunoelectrophoresis reference patterns. Extensive studies on the antigenic structure of membrane vesicles isolated from *E. coli* and grown aerobically on succinate (succinate-oxygen vesicles) have yielded valuable information about the structural properties of these membrane vesicles (32–34). The protein composition of aerobic membranes differs considerably from that of membranes obtained from anaerobically grown *E. coli* (39). The crossed immunoelectrophoresis reference patterns from gluocse-

TABLE 1. Characterization of precipitation lines in the reference patterns for glucose-nitrate and glycerol-fumarate vesicles of *E. coli* ML308-225

Vesicles	Precipitation line no.	Enzyme activity
Glucose-nitrate	13	6-Phosphogluconate dehydrogenase
	15	ATPase
	41,42	NADH dehydrogenase
	44	Nitrate reductase; formate dehydrogenase[a]
	54	Formate dehydrogenase
	61	Dihydroorotate dehydrogenase
	63	D-Lactate dehydrogenase
Glycerol-fumarate	5	6-Phosphogluconate dehydrogenase
	11	Cytochrome oxidase
	15	ATPase
	16	NADH dehydrogenase
	25 plus 43	Fumarate reductase
	35	Nitrate reductase
	37,38	Hydrogenase
	40	Malate dehydrogenase
	44	Glycerol-3-phosphate dehydrogenase
	45	D-Lactate dehydrogenase
	46	Succinate dehydrogenase

[a] Minor formate dehydrogenase activity.

nitrate vesicles and from glycerol-fumarate vesicles were first composed.

Treatment of the membrane vesicles with Triton X-100 (see above) resulted in the solubilization of 60 to 80% of the membrane protein, and typical immunoplates were obtained when glucose-nitrate vesicle proteins (Fig. 1A) or glycerol-fumarate vesicle proteins (Fig. 1B) were electrophoresed against their respective antibodies. Reference patterns of glucose-nitrate membrane vesicles (Fig. 2A) and glycerol-fumarate membrane vesicles (Fig. 2B) were derived from a series of immunoplates run with 100-fold variations in antibody concentration. The number of detectable immunoprecipitates was 83 for glucose-nitrate vesicles and 70 for glycerol-fumarate vesicles. Proteins migrating towards the cathode (pI > 8.6) were detected; these have also been observed in succinate-oxygen vesicles (33).

Characterization of immunoprecipitates. Zymogram staining techniques have been used to identify the precipitation lines of succinate-oxygen membrane vesicles (32, 33), and this technique was applied and extended to identify precipitation lines in the reference patterns of Fig. 2 (Table 1). The most relevant zymograms are shown in Fig. 3.

In glucose-nitrate vesicles, nitrate reductase (Fig. 2A and Table 1, line 44), formate dehydrogenase (lines 54 and 44), and ATPase (line 15) activities were identified (Fig. 3), but hydrogenase was absent. Nitrate reductase was identified by the nitrate-dependent oxidation of reduced methyl viologen (Fig. 3A), and its assignment to precipitation line 44 was confirmed by staining the nitrite formed upon nitrate reduction with sulfanilamide (Fig. 3B). No fumarate reduction activity was detected in the immunoplates of glucose-nitrate vesicles, and this is consistent with the fact that fumarate reductase is repressed during growth in the presence of nitrate (2). Formate dehydrogenase activity was found in precipitation line 54 and weakly in line 44, the nitrate reductase line. Moreover, the latter contained formate nitrate oxidoreductase activity, as indicated by the formation of nitrite upon the addition of formate and nitrate (data not shown). This suggests that in the Triton X-100 solubilizate, some enzyme complexes have retained the supramolecular organization present in intact membranes.

In glycerol-fumarate vesicles, hydrogenase (Fig. 2B and Table 1, line 37), fumarate reductase (lines 25 plus 43), ATPase (line 15), glycerol-3-phosphate dehydrogenase, and nitrate reductase (line 35) were identified (Fig. 4). Fumarate reductase was found in two fused precipitation lines, indicating the presence of identical antigenic determinants in the two complexes. The relative amounts of material in the two fused peaks varied with the Triton X-100 concentration used for solubilization. The component having the lower mobility increased with increasing Triton X-100 concentrations. These results also indicate the presence of supramolecular aggregates in the Triton X-100 solubilizate. However, attempts to dissociate these complexes, as has been done for the NADH dehydrogenase complexes of *Bacillus subtilis* (1), failed because fumarate reductase was inactivated by sodium dodecyl sulfate at concentrations as low as 0.1% (wt/vol). Nitrate reductase was also present in these vesicles, but in much smaller quantity than in glucose-nitrate vesicles. This is consistent with induction of the reductase by nitrate (18, 25). Glycerol-3-phosphate dehydrogenase activity was associated with only one precipitation line (Fig. 2B, line 44). This is probably the anaerobic enzyme formed under conditions of fumarate reduction rather than the aerobic enzyme, which predominates when O_2 or nitrate serves as terminal electron acceptor (10, 24). Two different hydrogenase activities

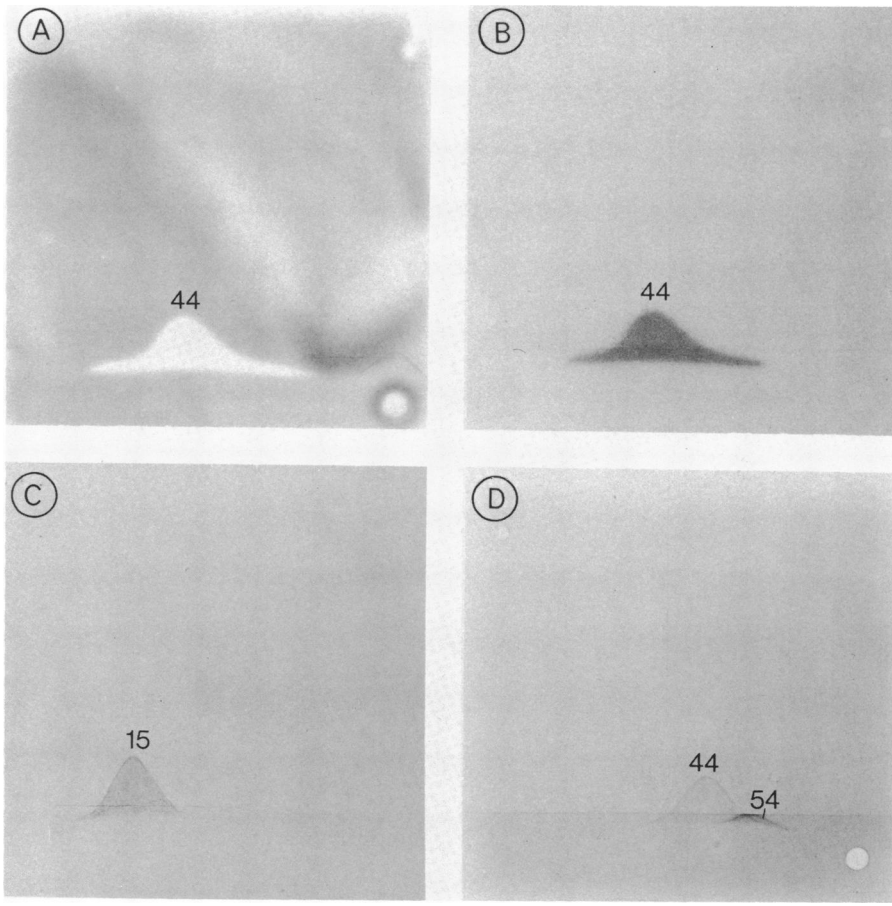

FIG. 3. Zymogram identification of nitrate reductase, formate dehydrogenase, and the membrane-bound ATPase complex in crossed immunoplates of glucose-nitrate vesicles. Gels similar to that shown in Fig. 1A were stained for nitrate reductase (A, precipitation line 44), nitrite formation (B, line 44), ATPase (C, line 15), and formate dehydrogenase (D, lines 54 and 44) as described in the text.

were observed. One of these (line 37) catalyzed the reversible transfer of electrons between H_2 and methyl viologen or benzyl viologen (Fig. 4A). The same line was permanently stained by the formation of an insoluble brown formazan from tetranitro blue tetrazolium with reduced viologen (see above), and this revealed a second hydrogenase activity (Fig. 2B, line 38). Line 38 lies completely under precipitation line 37 in the reference pattern, but under other conditions the lines intersected. The position and form of line 37 are similar to those found by Graham et al. (15), who detected only one hydrogenase activity. Other enzymes that were identified are listed in Table 1.

Assignment of the immunoprecipitates of fumarate reductase. The immunoprecipitates corresponding to fumarate reductase were assigned by studies with mutants lacking or overproducing fumarate reductase and the purified enzyme. The vesicles of the parental strain (JRG653, *frd*$^+$ *sdh*$^+$) resembled those of ML308-225 in possessing two major fused immunoprecipitates (Fig. 2B, lines 25 plus 43) staining for succinate oxidation activity (Fig. 4B and 5B). A minor component (line 46) was also detected (Fig. 5B). Formazan formation by the major precipitates became visible after 4 h and was complete at 24 h, by which time the minor line was only just detectable. Only one of these three immunoprecipitates (line 43) exhibited weak fumarate reduction activity by the methyl viologen assay.

Crossed immunoelectrophoresis of purified fumarate reductase against glycerol-fumarate antibodies showed only one immunoprecipitate with succinate oxidation activity, and this corresponded to one of the two fused immunoprecipitates (Fig. 2B, line 25; Fig. 5A). Tandem-crossed and cocrossed electrophoresis confirmed this assignment. Furthermore, when glycerol-fuma-

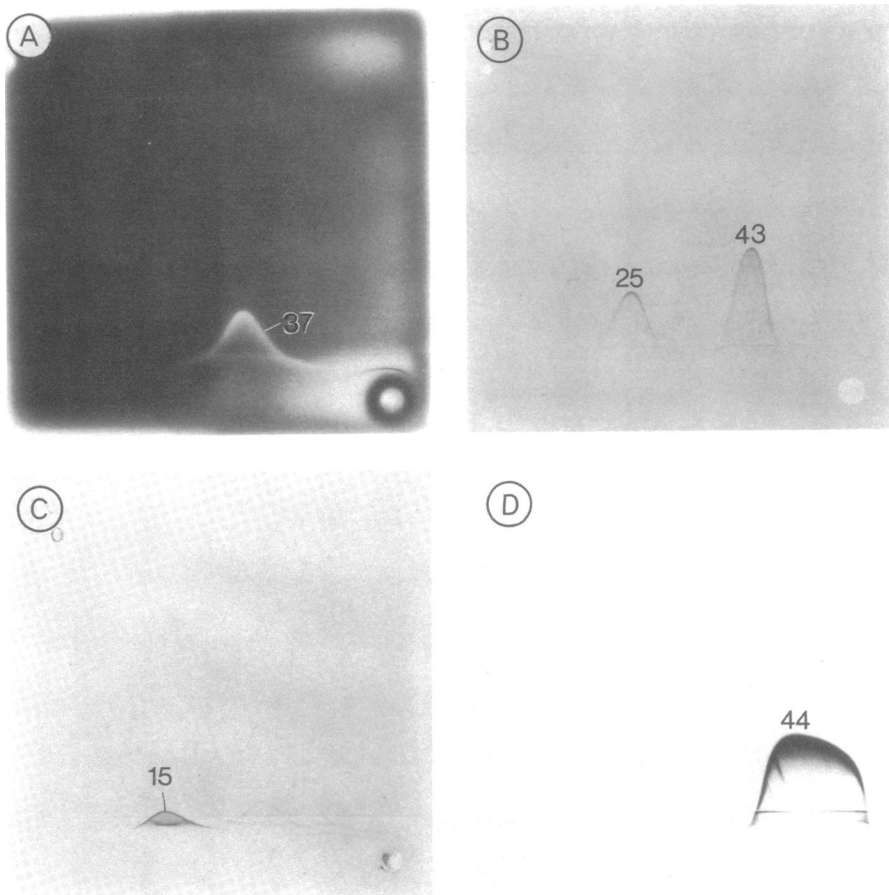

FIG. 4. Zymogram identification of fumarate reductase, hydrogenase, glycerol-3-phosphate dehydrogenase, and ATPase in crossed immunoelectrophoresis gels of glycerol-fumarate vesicles. Gels similar to that shown in Fig. 1B were stained for hydrogenase (A, precipitation line 37), fumarate reductase (by means of succinate oxidation activity) (B, lines 25 plus 43), ATPase (C, line 15) and glycerol-3-phosphate dehydrogenase (D, line 44) as described in the text.

rate antibodies were adsorbed with purified enzyme, both precipitation lines (Fig. 2B, lines 25 and 43) disappeared from the immunoprecipitation pattern.

The mutant and parental strains were all grown on a glucose-fumarate medium because it permits growth of the *frd* amber mutant, promotes full derepression of the fumarate reductase system (compare Fig. 5B with Fig. 4B), and provides membrane vesicles that are directly comparable. Crossed immunoelectropherograms stained for succinate oxidation activity clearly showed that the two fused immunoprecipitates are completely absent in the *frd* amber mutant (Fig. 5C). Moreover, the left-hand component (Fig. 5D, line 25) was significantly enlarged in the overproducing strain. This is consistent with an increased level of this antigen in these membranes. Adsorption of the glycerol-fumarate antibodies with purified fumarate reductase specifically removed the two fused precipitates, but the minor succinate oxidation activity was unaffected. By contrast, adsorption with solubilized membranes of the *frd* mutant specifically removed the minor activity and left the major activity completely unchanged (data not shown). These results show that antigens 25 and 43 correspond to fumarate reductase. The minor activity (antigen 46) would thus appear to be succinate dehydrogenase. The position of this precipitate relative to ATPase corresponds to the position of succinate dehydrogenase found by Smyth et al. (38) in aerobically grown *E. coli* K-12. However, totally different positions of two succinate dehydrogenase activities were found by Condon and Owen (6) in *E. coli* ML308-225 grown aerobically on succinate. This discrepancy was not investigated further.

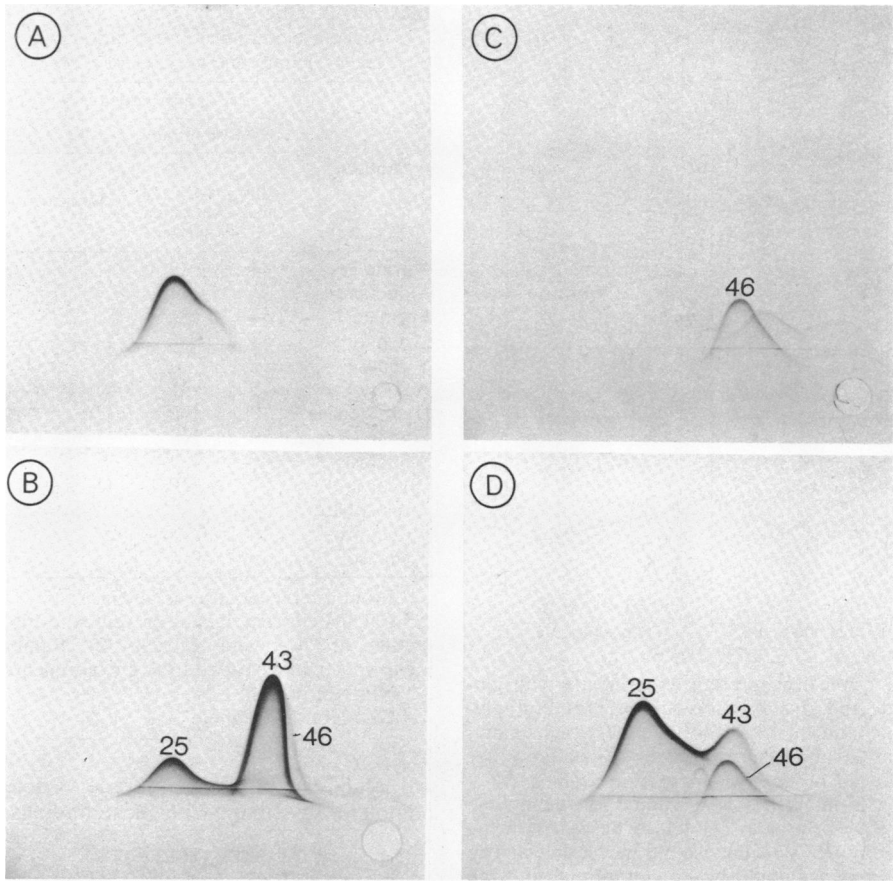

FIG. 5. Identification of immunoprecipitates corresponding to fumarate reductase by crossed immunoelectrophoresis with the purified enzyme and with solubilized membranes of mutant strains of *E. coli* K-12 grown on glucose-fumarate medium. Fumarate reductase alone (A; 5 μg of purified protein) and EDTA–Triton X-100 extracts of *E. coli* K-12 strains (B through D; 54 μg of membrane protein) were analyzed against 8.8 mg of glycerol-fumarate antibodies in the crossed immunoelectrophoresis system. The resulting immunoplates were all stained for succinate oxidation activity. (A) Purified fumarate reductase; (B) parental strain (JRG653, *frd*$^+$ *sdh*$^+$); (C) fumarate reductase amber mutant (JRG531, *frd*$^-$ *sdh*$^+$); (D) fumarate reductase overproducer (JRG1030, *frd*$_n^+$ *sdh*$^+$).

It is important to stress that with crossed immunoelectrophoresis it is possible to quantitate the succinate dehydrogenase and fumarate reductase in a single preparation (compare ref. 37). This could be very helpful in studies on the genetic regulation of these two enzymes.

Localization of reductases and dehydrogenases in membrane vesicles. Information about the localization of enzymes in membrane vesicles relative to the hydrophobic barrier can be obtained from immunoadsorption studies (1, 9, 32, 34; see above). Accordingly, this technique was applied to ATPase, formate dehydrogenase, and nitrate reductase from glucose-nitrate vesicles and to ATPase, hydrogenase, glycerol-3-phosphate dehydrogenase, and fumarate reductase from glycerol-fumarate vesicles. In all cases, the enzymes were located relative to ATPase, which is known to be at the cytoplasmic side of the membrane (32).

The accessibility of the respective antigens is reflected by the slopes of the lines relating the inverse peak area to the amount of antigen added (32). By comparing the slopes of the lines obtained with disrupted and intact membrane vesicles, the relative expression of an antigen at the external surface of the membrane can be calculated. Typical results are illustrated in Fig. 6 and summarized in Table 2. It can be concluded that hydrogenase, glycerol-3-phosphate dehydrogenase, nitrate reductase, and both fumarate reductase components are, like ATPase, located at the cytoplasmic side of the vesicle membrane. Formate dehydrogenase exhibits a

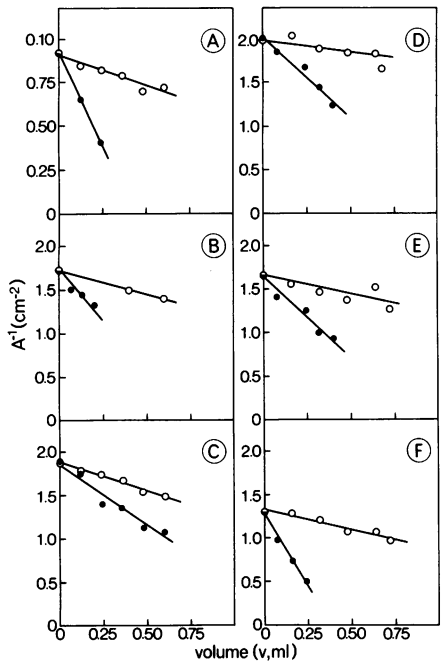

FIG. 6. Typical adsorption experiments with glucose-nitrate and glycerol-fumarate vesicles. Anti-glucose-nitrate- and anti-glycerol-fumarate-vesicle immunoglobulins (28 and 39 mg of protein, respectively, per 1 ml) were adsorbed with increasing volumes of a suspension of intact (○) or disrupted (●) membrane vesicles (5 mg of protein per ml) as described in the text. (A through C) Glucose-nitrate vesicles. The absorbed immunoglobulin was incorporated into the second dimension agarose gel (100 μl for A, 50 μl for B and C) and was analyzed against an EDTA–Triton X-100 extract of membrane vesicles (37 μg of protein). (D through F) Glycerol-fumarate vesicles. The absorbed immunoglobulin was incorporated into the second-dimension agarose gel (200 μl) and was analyzed against an EDTA–Triton X-100 extract of membrane vesicles (43 μg of protein for D and E, 36 μg for F). The reciprocal peak area of the resulting immunoprecipitates (A^{-1}) is plotted against the volume (v) of the vesicle suspension used. (A) Nitrate reductase (precipitation line 44); (B) ATPase (line 15); (C) formate dehydrogenase (line 54); (D) hydrogenase (line 37); (E) ATPase (line 15); (F) fumarate reductase (lines 25 plus 43).

behavior which is characteristic of transmembrane proteins.

Several different methods have been used to show that in *E. coli*, nitrate reductase is located at the inner side of the membrane of intact cells (3, 13, 21), and this conclusion has recently been confirmed by immunoadsorption studies with spheroplasts of *E. coli* (16). A transmembranal location of formate dehydrogenase in *E. coli* has been demonstrated by several methods, including immunoadsorption with spheroplasts (14, 16). Our results with membrane vesicles are in complete agreement with these findings.

TABLE 2. Orientation of enzymes of the fumarate reductase and nitrate respiration systems in membrane vesicles of *E. coli*

Antigen	Orientation in vesicles			
	Glucose-nitrate		Glycerol-fumarate	
	Line no.[a]	% Exposed at outer surface[b]	Line no.[a]	% Exposed at outer surface[b]
Nitrate reductase	44	19		ND[d]
Formate dehydrogenase	54	51		ND
ATPase	15	31	15	24
Hydrogenase		NP[c]	37	26
Fumarate reductase		NP	25 plus 43	15
Glycerol-3-phosphate dehydrogenase		NP	44	28

[a] From reference patterns in Fig. 2.
[b] Calculated from data as presented in Fig. 6 by the method of Owen and Kaback (32). Numbers show mean values of from two to five experiments.
[c] NP, Not present.
[d] ND, Not determined.

LITERATURE CITED

1. **Bergsma, J., R. Strijker, J. Y. E. Alkema, H. G. Seijen, and W. N. Konings.** 1981. NADH dehydrogenase and NADH oxidation in membrane vesicles from *Bacillus subtilis*. Eur. J. Biochem. **120**:599–606.
2. **Boonstra, J., M. T. Huttunen, W. N. Konings, and H. R. Kaback.** 1975. Anaerobic transport in *Escherichia coli* membrane vesicles. J. Biol. Chem. **250**:6792–6798.
3. **Boxer, D. H., and R. A. Clegg.** 1975. A transmembrane-location for the proton-translocating reduced ubiquinone-nitrate reductase segment of the respiratory chain of *Escherichia coli*. FEBS Lett. **60**:54–57.
4. **Burstone, M. S.** 1959. New histochemical techniques for the demonstration of tissue oxidase (cytochrome oxidase). J. Histochem. Cytochem. **7**:112–122.
5. **Cole, S. T., and J. R. Guest.** 1979. Production of a soluble form of fumarate reductase by multiple gene duplication in *Escherichia coli* K12. Eur. J. Biochem. **102**:65–71.
6. **Condon, C., and P. Owen.** 1981. Characterization of succinate dehydrogenase from *Escherichia coli*. Soc. Gen. Microbiol. Q. **8**:116.
7. **Dickie, P., and J. H. Weiner.** 1979. Purification and characterization of membrane-bound fumarate reductase from anaerobically grown *Escherichia coli*. Can. J. Biochem. **57**:813–821.
8. **Dully, J. R., and P. A. Grieve.** 1975. A simple technique for eliminating interference by detergents in the Lowry method of protein determination. Anal. Biochem. **64**:136–141.
9. **Elferink, M. G. L., K. J. Hellingwerf, P. A. M. Michels, H. G. Seijen, and W. N. Konings.** 1979. Immunochemical analysis of membrane vesicles and chromatophores of *Rhodopseudomonas sphaeroides* by crossed immunoelectrophoresis. FEBS Lett. **107**:300–307.
10. **Freedberg, W. B., and E. C. C. Lin.** 1973. Three kinds of

controls affecting the expression of the *glp* regulon in *Escherichia coli*. J. Bacteriol. **115**:816–823.
11. **Garland, P. B., J. A. Downie, and B. A. Haddock.** 1975. Proton translocation and the respiratory nitrate reductase of *Escherichia coli*. Biochem. J. **152**:547–559.
12. **Ghosh, R., and J. R. Quayle.** 1979. Phenazine ethosulfate as a preferred electron acceptor to phenazine methosulfate in dye-linked enzyme assays. Anal. Biochem. **99**:112–117.
13. **Graham, A., and D. H. Boxer.** 1978. Immunochemical localization of nitrate reductase in *Escherichia coli*. Biochem. Soc. Trans. **6**:1210–1211.
14. **Graham, A., and D. H. Boxer.** 1981. The organization of formate dehydrogenase in the cytoplasmic membrane of *Escherichia coli*. Biochem. J. **195**:627–637.
15. **Graham, A., D. H. Boxer, B. A. Haddock, M. A. Mandrand-Berthelot, and R. W. Jones.** 1980. Immunochemical analysis of the membrane-bound hydrogenase of *Escherichia coli*. FEBS Lett. **113**:167–172.
16. **Graham, A., A. D. Tucker, and N. H. Smith.** 1981. The formate-nitrate respiratory chain of *Escherichia coli*: localisation of proteins by immunoadsorption studies. FEMS Microbiol. Lett. **11**:141–147.
17. **Gutowski, S. J., and H. Rosenberg.** 1976. Effects of dicyclohexylcarbodiimide on proton translocation coupled to fumarate reduction in anaerobically grown cells of *Escherichia coli* K12. Biochem. J. **160**:813–816.
18. **Haddock, B. A., and C. W. Jones.** 1977. Bacterial respiration. Bacteriol. Rev. **41**:47–99.
19. **Hellingwerf, K. J., J. G. M. Bolscher, and W. N. Konings.** 1981. The electrochemical proton gradient generated by the fumarate-reductase system in *Escherichia coli* and its bioenergetic implications. Eur. J. Biochem. **113**:369–374.
20. **Hirsch, C. A., M. Rasminsky, B. D. Davis, and E. C. C. Lin.** 1963. A fumarate reductase in *Escherichia coli* distinct from succinate dehydrogenase. J. Biol. Chem. **238**:3770–3774.
21. **Jones, R. W., and P. B. Garland.** 1977. Site and specificity of the reaction of bipyridylium compounds with anaerobic respiratory enzymes of *Escherichia coli*: effects of permeability barriers imposed by the cytoplasmic membrane. Biochem. J. **164**:199–211.
22. **Jones, R. W., A. Lamont, and P. B. Garland.** 1980. The mechanism of proton translocation driven by the respiratory nitrate reductase complex of *Escherichia coli*. Biochem. J. **190**:79–94.
23. **Joustra, M., and H. Lundgren.** 1969. Preparation of freeze-dried monomeric and immunochemically pure IgG by a rapid and reproducible chromatographic technique. Protides Biol. Fluids Proc. Colloq. **17**:511–515.
24. **Kistler, W. S., C. A. Hirsch, N. R. Cozzarelli, and E. C. C. Lin.** 1969. Second pyridine nucleotide-independent L-α-glycerophosphate dehydrogenase in *Escherichia coli* K-12. J. Bacteriol. **100**:1133–1135.
25. **Konings, W. N., and J. Boonstra.** 1977. Anaerobic electron transfer and active transport in bacteria. Curr. Top. Membr. Transp. **9**:177–231.
26. **Konings, W. N., and H. R. Kaback.** 1973. Anaerobic transport in *Escherichia coli* membrane vesicles. Proc. Natl. Acad. Sci. U.S.A. **70**:3376–3381.
27. **Kröger, A.** 1980. Bacterial electron transport to fumarate, p. 1–17. *In* C. J. Knowles (ed.), Diversity of bacterial respiratory systems, vol. 2. CRC Press, Boca Raton, Fla.
28. **Lowry, O. H., N. J. Rosebrough, A. J. Farr, and R. J. Randall.** 1951. Protein measurement with the Folin phenol reagent. J. Biol. Chem. **193**:265–275.
29. **Lund, K., and J. A. DeMoss.** 1976. Association-dissociation behavior and subunit structure of heat-released nitrate reductase from *Escherichia coli*. J. Biol. Chem. **251**:2207–2216.
30. **Miki, K., and E. C. C. Lin.** 1973. Enzyme complex which couples glycerol-3-phosphate dehydrogenation to fumarate reduction in *Escherichia coli*. J. Bacteriol. **114**:767–771.
31. **Miki, K., and T. H. Wilson.** 1978. Proton translocation associated with anaerobic transhydrogenation from glycerol-3-phosphate to fumarate in *Escherichia coli*. Biochem. Biophys. Res. Commun. **83**:1570–1575.
32. **Owen, P., and H. R. Kaback.** 1978. Molecular structure of membrane vesicles from *Escherichia coli*. Proc. Natl. Acad. Sci. U.S.A. **75**:3148–3152.
33. **Owen, P., and H. R. Kaback.** 1979. Immunochemical analysis of membrane vesicles from *Escherichia coli*. Biochemistry **18**:1413–1422.
34. **Owen, P., and H. R. Kaback.** 1979. Antigenic architecture of membrane vesicles from *Escherichia coli*. Biochemistry **18**:1422–1426.
35. **Owen, P., and M. R. J. Salton.** 1975. Antigenic and enzymatic architecture of *Micrococcus lysodeikticus* membranes established by crossed immunoelectrophoresis. Proc. Natl. Acad. Sci. U.S.A. **72**:3711–3715.
36. **Sánchez Crispín, J. A., M. Dubourdieu, and M. Chippaux.** 1979. Localization and characterization of cytochromes from membrane vesicles of *Escherichia coli* K12 grown in anaerobiosis with nitrate. Biochim. Biophys. Acta **547**:198–210.
37. **Skovbjerg, H.** 1981. Immunoelectrophoretic studies on human small-intestinal brush-border proteins. Biochem. J. **193**:887–890.
38. **Smyth, C. J., J. Siegel, M. R. J. Salton, and P. Owen.** 1978. Immunochemical analysis of inner and outer membranes of *Escherichia coli* by crossed immunoelectrophoresis. J. Bacteriol. **133**:306–319.
39. **Spencer, M. E., and J. R. Guest.** 1974. Proteins of the inner membrane of *Escherichia coli*: changes in composition associated with anaerobic growth and fumarate reductase amber mutation. J. Bacteriol. **117**:954–959.
40. **Stouthamer, A. H., J. van't Riet, and L. F. Oltmann.** 1980. Respiration with nitrate as acceptor, p. 19–48. *In* C. J. Knowles (ed.), Diversity of bacterial respiratory systems, vol. 2. CRC Press, Boca Raton, Fla.
41. **Ten Brink, B., and W. N. Konings.** 1980. Generation of an electrochemical proton gradient by lactate efflux in membrane vesicles of *Escherichia coli*. Eur. J. Biochem. **111**:59–66.
42. **Thomas, P. E., D. Ryan, and W. Levin.** 1976. An improved staining procedure for the detection of the peroxidase activity of cytochrome P-450 on sodium dodecyl sulfate polyacrylamide gels. Anal. Biochem. **75**:168–176.
43. **Weiner, J. H., and P. Dickie.** 1979. Fumarate reductase of *Escherichia coli*: elucidation of the covalent-flavin component. J. Biol. Chem. **254**:8590–8593.